BIOCHEMISTRY
including biophysical chemistry & molecular biology

Article

pubs.acs.org/biochemistry

Site-Directed Mutagenesis Maps Interactions That Enhance Cognate and Limit Promiscuous Catalysis by an Alkaline Phosphatase Superfamily Phosphodiesterase

Helen Wiersma-Koch, Fanny Sunden, and Daniel Herschlag*

Department of Biochemistry, Stanford University, Stanford, California 94305, United States

Supporting Information

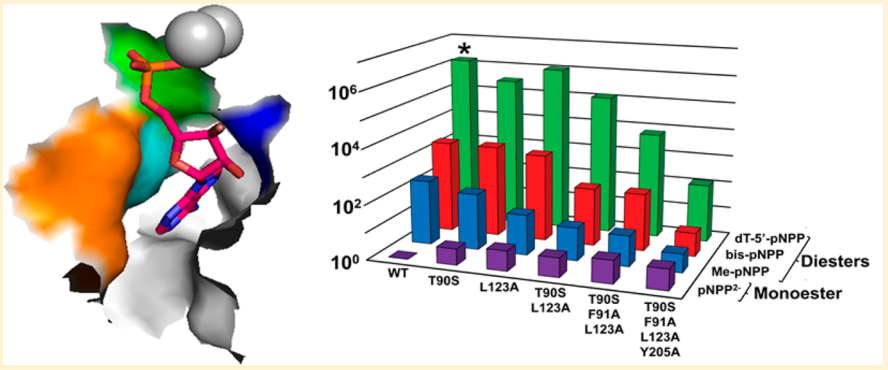

ABSTRACT: Catalytic promiscuity, an evolutionary concept, also provides a powerful tool for gaining mechanistic insights into enzymatic reactions. Members of the alkaline phosphatase (AP) superfamily are highly amenable to such investigation, with several members having been shown to exhibit promiscuous activity for the cognate reactions of other superfamily members. Previous work has shown that nucleotide pyrophosphatase/phosphodiesterase (NPP) exhibits a >10^6-fold preference for the hydrolysis of phosphate diesters over phosphate monoesters, and that the reaction specificity is reduced 10^3-fold when the size of the substituent on the transferred phosphoryl group of phosphate diester substrates is reduced to a methyl group. Here we show additional specificity contributions from the binding pocket for this substituent (herein termed the R′ substituent) that account for an additional ∼250-fold differential specificity with the minimal methyl substituent. Removal of four hydrophobic side chains suggested on the basis of structural inspection to interact favorably with R′ substituents decreases phosphate diester reactivity 10^4-fold with an optimal diester substrate (R′ = 5′-deoxythymidine) and 50-fold with a minimal diester substrate (R′ = CH_3). These mutations also enhance the enzyme's promiscuous phosphate monoesterase activity by nearly an order of magnitude, an effect that is traced by mutation to the reduction of unfavorable interactions with the two residues closest to the nonbridging phosphoryl oxygen atoms. The quadruple R′ pocket mutant exhibits the same activity toward phosphate diester and phosphate monoester substrates that have identical leaving groups, with substantial rate enhancements of ∼10^{11}-fold. This observation suggests that the Zn^{2+} bimetallo core of AP superfamily enzymes, which is equipotent in phosphate monoester and diester catalysis, has the potential to become specialized for the hydrolysis of each class of phosphate esters via addition of side chains that interact with the substrate atoms and substituents that project away from the Zn^{2+} bimetallo core.

Catalytic promiscuity likely provided the starting point in the evolution of new enzymes with new functions. Most generally, a low level of activity of a gene-duplication product can provide a head start toward the selection of a new, beneficial activity, and the optimization process can be guided by natural selection as soon as its activity increases to a level sufficient to provide a selective advantage.[1,2] Catalytic promiscuity is also a powerful functional tool that can be exploited in uncovering differences among enzyme families that lead to functional differences in reaction specificity and in uncovering their mechanistic origins.[3−8] This comparative enzymology approach has been effectively used in studies of the alkaline phosphatase (AP) superfamily, the members of which catalyze a range of phosphoryl and sulfuryl transfer reactions.[9−18] One of the more well-studied enzymes in the AP superfamily, nucleotide pyrophosphatase/phosphodiesterase (NPP), catalyzes phosphate diester hydrolysis and possesses catalytic promiscuity for phosphate monoester and sulfate monoester hydrolysis.[15,17,19] Here we use comparative enzymology, assessing the reactions of NPP with phosphate diester and phosphate monoester substrates, to further probe how this enzyme achieves its reaction specificity for phosphate diesters over monoesters.

Received: July 25, 2013
Revised: October 31, 2013
Published: November 21, 2013

dx.doi.org/10.1021/bi4010045 | *Biochemistry* 2013, 52, 9167−9176

A common conserved feature in the main group of the AP superfamily is a bimetallo site (Figure 1).[9] These enzymes have phosphomonoesterase, phosphodiesterase, phosphomutase, and phosphonoacetate hydrolase activity.[12,13,17,20] NPPs constitute a large phosphodiesterase subgroup in this family.[21] While NPP shares a Zn^{2+} bimetallo motif with other superfamily members, its other active site features are distinct from those of the other well-characterized members of this subgroup of the AP superfamily (Figure 1).[12,17,20] All of the enzymes in the main branch of the AP superfamily place one of the oxygen atoms of the transferred phosphoryl group between the metal ions of the bimetallo site. However, whereas other members of the AP superfamily transfer an unsubstituted phosphoryl group ($-PO_3^{2-}$) and donate hydrogen bonds to both of the nonbridging phosphoryl oxygen atoms of monoester substrates, NPP transfers a substituted phosphoryl group ($-PO_2OR'^-$) and has a substituent binding pocket that interacts with the R′ substituent attached to one of the phosphoryl oxygen atoms of its diester substrates (Figure 1).[17,22−24] This pocket functionally replaces one set of hydrogen bonds that provide favorable interactions with monoester substrates in the monoesterase members of the superfamily. Depending on the architecture of the pocket, substrates for enzymes in the NPP family can be nucleotides or lipids, such as choline phosphoesters, and sphingomyelin.[17,21,24−29]

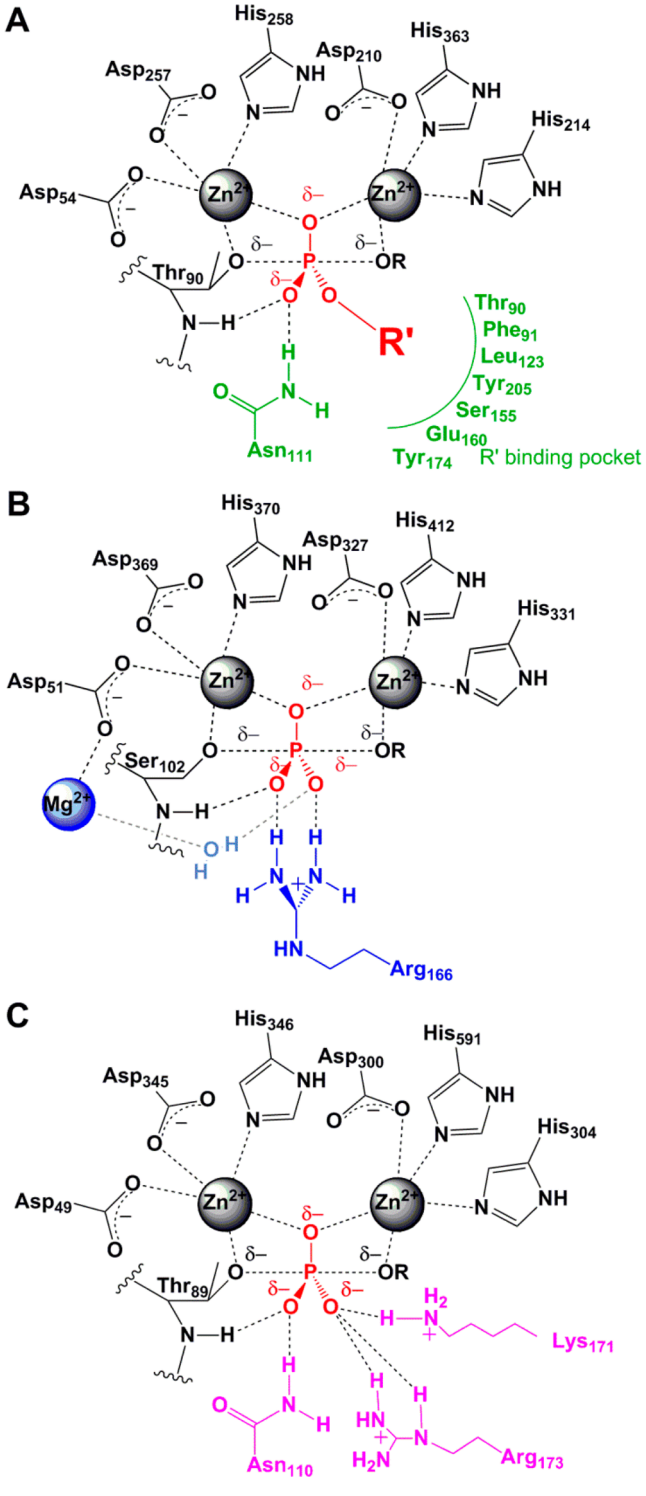

Figure 1. Comparison of the active sites of three members of the alkaline phosphatase superfamily, the diesterase NPP (*Xanthomonas axonopodis* pv. *citri*) (A), the monoesterase AP (*Escherichia coli* alkaline phosphatase) (B), and the monoesterase SPAP (*Sphingomonas* sp. strain BSAR-1 alkaline phosphatase) (C). Colored red is a transition state model of the transferred phosphoryl. Colored black is the conserved bimetallo core, whereas features unique to each are shown in different colors.

The different active site features at this position are presumably responsible for at least some of the reaction specificity of NPP for phosphate diesters. Previous work determined that diester substrates with large R′ substituents react 10^3-fold faster than the corresponding diester with a methyl substituent (Chart 1) or monoester monoanion that has a hydrogen atom at the corresponding position. Consistent with these observations, an NPP X-ray structure with bound AMP revealed the presence of a recognition pocket (the R′ pocket).[17] Here we further probe the effects of this recognition pocket, combining variation in the identity of the R′ substituent of diester substrates, Me-pNPP, bis-pNPP, and dT-5′-pNPP, with mutagenesis of residues within the R′ pocket, and comparison to reaction of the corresponding phosphate monoester substrate, pNPP (Chart 1). We identify roles for each of the four residues at the mouth of the R′ pocket, and the results further suggest that the AP superfamily bimetallo core provides substantial and equal catalysis for reactions of phosphate monoesters and diesters.

MATERIALS AND METHODS

Protein Expression and Purification. NPP from *Xanthomonas axonopodis* pv. *citri* was purified from a construct containing an N-terminal maltose binding protein (MBP) fusion and C-terminal strepII tags with a Factor Xa cleavage site between it and the natural C-terminal end of NPP.[30−32] This protein was expressed from a pMal-p2X vector that also contains the coding regions for an N-terminal signal peptide sequence for periplasmic export upstream of the MBP coding region (Figure S1 of the Supporting Information). Control experiments with wild-type NPP showed that NPP with tags removed and NPP containing the purification tags had the same monoesterase and diesterase activity as previously reported for wild-type NPP. Hence, the tags were retained in the experiments presented herein. Evidence that NPP was responsible for all of the observed activities was provided by the observation that mutation of the nucleophilic threonine to glycine (T90G) gave no measurable activity; additional evidence that the monoesterase and diesterase activities arise from the same NPP active sites was provided by the

dx.doi.org/10.1021/bi4010045 | *Biochemistry* 2013, 52, 9167−9176

Chart 1. Substrates Used in This Study

Phosphate Monoesters

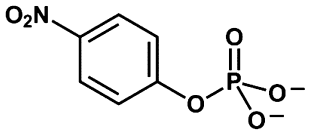

p-nitrophenyl phosphate dianion ($pNPP^{2-}$)

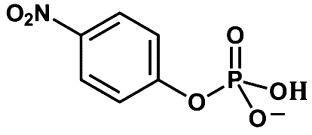

p-nitrophenyl phosphate monoanion ($pNPP^{1-}$: diester analogue herein)

Phosphate Diesters (monoanion)

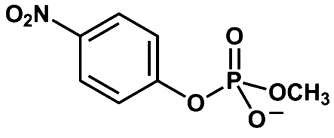

methyl-*p*-nitrophenyl phosphate (Me-pNPP)

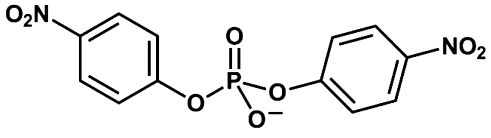

bis-*p*-nitrophenyl phosphate (bis-pNPP)

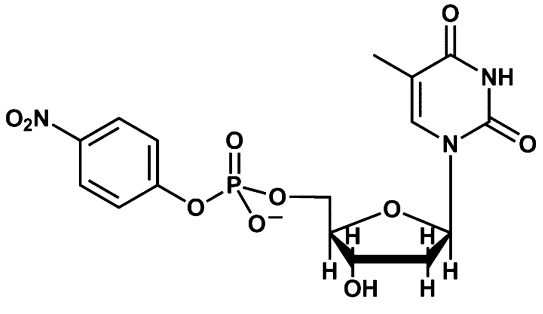

deoxythymidine-5'-*p*-nitrophenyl phosphate (dT-5'-pNPP)

observation of common inhibition constants, as described below.

Escherichia coli SM547(DE3) cells containing the MBP-NPP-strepII construct were grown to an optical density of 0.6 in rich medium and glucose (10 g of tryptone, 5 g of yeast extract, 5 g of NaCl, and 2 g of glucose per liter) with 50 μg/mL carbenicillin at 37 °C. Isopropyl thiogalactopyranoside was added to a final concentration of 0.3 mM to induce protein expression. Cultures were then grown at 30 °C for 16−20 h.

For the T90S/L123A, T90S/F91A/L123A, and T90S/F91A/L123A/Y205A mutants, cells were harvested by centrifugation and lysed via osmotic shock. Briefly, the cell pellet was resuspended in 800 mL of a 20% sucrose solution [30 mM Tris-HCl (pH 8.0) and 1 mM EDTA] and incubated at room temperature for 10 min. The cells were pelleted and resuspended in 800 mL of ice-cold water. Following a 10 min incubation at 4 °C and centrifugation, the supernatant was adjusted to 10 mM Tris-HCl (pH 8.0) with 10 μM $ZnCl_2$. The sample was then passed over a 5 mL Q-Sepharose Fast Flow column (Amersham) to concentrate the large volume obtained from the osmotic shock. The column was washed with 2 column volumes of 0.01 M Tris-HCl (pH 8.0) and 2 column volumes of 0.1 M NaCl and 0.01 M Tris-HCl (pH 8.0). Protein was eluted with 10 mM Tris-HCl (pH 8.0) and 0.2 M NaCl. Tris-HCl (pH 8.0) was added to the eluate to a final concentration of 0.1 M, and the eluate was then loaded onto a 3 mL streptactin column (made in house[30]). The column was washed with 6 column volumes of wash buffer [100 mM Tris-HCl (pH 8.0) and 0.5 M NaCl]. Protein was then eluted with 2.5 mM desthiobiotin in wash buffer. Protein-containing fractions were concentrated to a volume of <1 mL by centrifugation through a 10 kDa cutoff filter (Amicon) and buffer exchanged two times into 10 mM sodium MOPS (pH 8.0), 50 mM NaCl, and 10 μM $ZnCl_2$.

For the T90S, F91A, L123A, and Y205A NPP mutants, cells were harvested by centrifugation and resuspended in 100 mM Tris-HCl (pH 8.0) and 150 mM NaCl. Cells were then lysed when the suspension was passed through an Emulsiflex (Avestin) three times. The lysate was clarified by centrifugation (20000*g* for 20 min), and the supernatant was filtered through a 0.45 μm filter. The protein solution was then loaded onto a 3 mL streptactin column as described above. For all enzymes, the purity was checked by sodium dodecyl sulfate−polyacrylamide gel electrophoresis and was >95% as estimated by staining with Coomassie Blue.[33] To test whether the purification method used for the single mutant produced sufficiently pure enzyme, the T90S/F91A/L123A mutant was expressed using either osmotic shock or the Emulsiflex to lyse the cells. The two purification techniques gave enzyme with activities that were the same within error.

Kinetic Assays. All rate constants herein were obtained using mutant varieties of the MBP-NPP-strepII construct. Reactions were performed in 0.1 M Tris-HCl (pH 8.0), 0.5 M NaCl, and 100 μM $ZnCl_2$ at 25 °C in a Perkin-Elmer UV/vis Lambda 25 spectrophotometer unless otherwise noted. All substrates contained *p*-nitrophenolate leaving groups (Chart 1), and the formation of *p*-nitrophenolate was monitored continuously at 400 nm[17] unless noted otherwise. Rate constants were determined from initial rates. The kinetic parameters were shown to be first-order in both enzyme and substrate, with concentrations of enzyme and substrate varied over an at least 10-fold range. The resulting data were linear with respect to enzyme or substrate concentration, with r^2 values of ≥0.98 in all cases. Thus, reactions were conducted under subsaturating conditions and provide measurements of k_{cat}/K_M. The following substrate concentrations were used: Me-pNPP and $pNPP^{2-}$, 0.06−1.0 mM for all enzymes; bis-pNPP, 0.06−1.0 mM for all enzymes except 0.03−2.2 mM for F91A; dT-5′-pNPP, 3.3−210 μM for T90S, 10−110 μM for F91A, 0.02−1.1 mM for L123A, 2.1−21 μM for Y205A, 0.01−2.5 mM for T90S/L123A, 1.0−50 μM for F91A/L123A, 0.03−2.2 mM for T90S/F91A/L123A, and 0.02−1.0 mM for T90S/F91A/

dx.doi.org/10.1021/bi4010045 | *Biochemistry* 2013, 52, 9167−9176

L123A/Y205A. In each case, a control reaction without enzyme was run and the background reaction was determined to be negligible. Inhibition constants for vanadate and tungstate were determined with subsaturating concentrations of substrate with the following ranges of inhibitor concentrations: T90S, 0.05−3.4 mM vanadate; L123A, 0.02−1.4 mM vanadate; F91A and Y205A, 0.04−1.4 mM tungstate; T90S/L123A, 0.04−1.3 mM tungstate; T90S/F91A/L123A and T90S/F91A/L123A/Y205A, 0.05−3.4 mM tungstate. The pH dependencies were determined with 0.1 M sodium MES (pH 6.0), 0.1 M sodium MOPS (pH 7.0), 0.1 M Tris-HCl (pH 8.0), and 0.1 M sodium CHES (pH 9.0), each in the presence of 0.5 M NaCl and 100 μM $ZnCl_2$ at 25 °C (Supporting Information). The observed diesterase activity requires release of *p*-nitrophenolate, as its absorbance is used to follow the reaction. As the measured diesterase reaction is faster than monoester hydrolysis in all cases except for the most mutated construct, the measured activities for these mutants cannot arise from first cleaving the R′ substituent to form a monoester intermediate, pNPP. In the case of the most mutated construct, the observed diesterase and monoesterase activities are similar, so that a lag would be expected if the observed hydrolysis proceeded through a monoester intermediate; no such lag is observed. When both substituents are *p*-nitrophenolate moieties (i.e., for bis-PNPP), small contributions to the observed reaction rate (up to 2-fold) can in principle arise from the subsequent hydrolysis of the pNPP that is formed, but simulations indicate that such contributions will be negligible for the enzymes studied herein.

Discontinuous assays for mono- and diester hydrolysis at low pH were performed in 0.1 M sodium MES (pH 4.7 and 5.0), each in the presence of 0.5 M NaCl and 100 μM $ZnCl_2$. The reactions were followed for 3000 min at 25 °C. At least eight aliquots (10 μL) of the reaction mixture were quenched in 5 μL of 1 M NaOH, and the absorbance was measured immediately. The absorbance recorded at 440 nm was subtracted from the absorbance recorded at 400 nm to account for changes in background from cuvette position or instrument fluctuations. Enzyme stability was assayed by diluting the enzyme reaction mixture 8-fold into 0.1 M Tris-HCl (pH 8.0), 0.5 M NaCl, 100 μM $ZnCl_2$, and 4.3 mM Me-pNPP. The formation of *p*-nitrophenolate was monitored continuously at 400 nm, and rate constants were determined via initial rates. Measured enzyme activities were within error of previously measured activities at pH 8.0, suggesting that the enzymes are stable at room temperature and pH 4.7 over this period of time.

RESULTS AND DISCUSSION

Seven residues make up the surface of the R′-binding pocket (Figure 2). The region of the pocket most remote from the bimetallo site contacts the nucleoside base and contains residues S155, E160, and Y174, and four other residues, T90, F91, L123, and Y205, make a hydrophobic halo of interactions at the mouth of the pocket (Figure 2 and Table 1). On the basis of the inspection of the X-ray structure of NPP with bound AMP,[17] we hypothesized that the residues at the mouth of this pocket provide favorable binding interactions even with the diester substrate containing only a methyl substituent and that these hydrophobic residues might additionally inhibit the monoesterase reaction because of their proximity to the partially negatively charged phosphoryl oxygen atom and ability to limit its solvation (Figure 2 and Table 1).

We first describe the effects of mutating the four residues at the mouth of the pocket on the diesterase reactions. We then

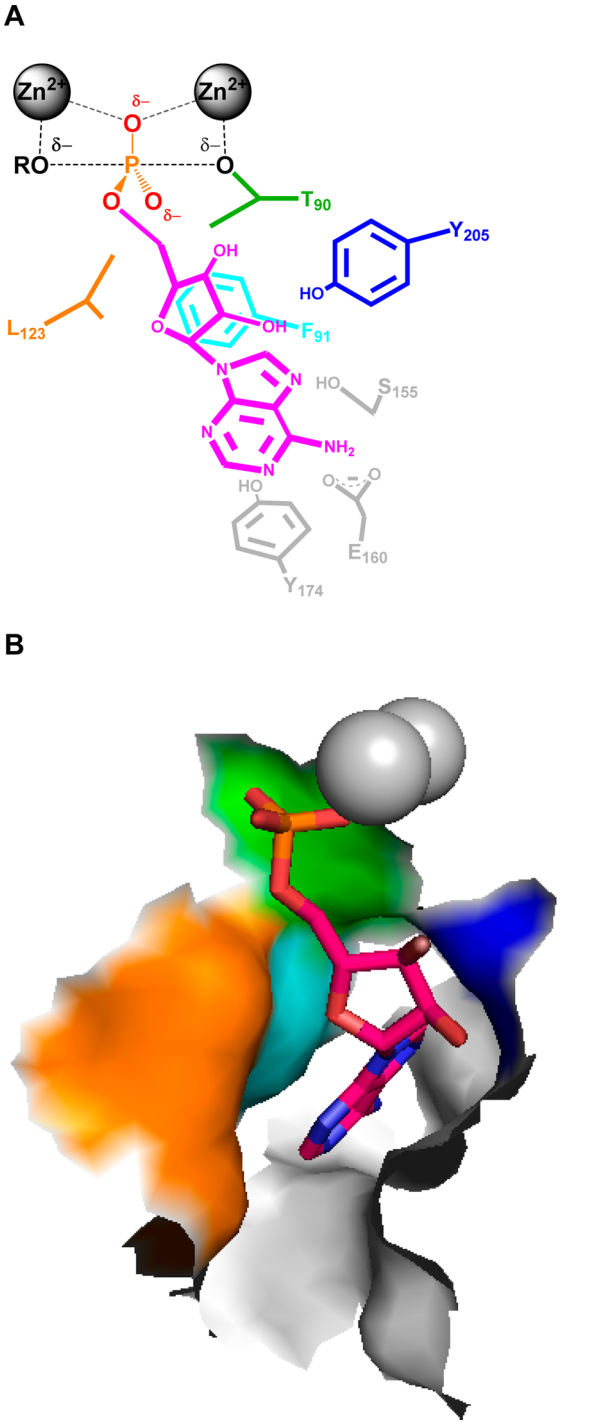

Figure 2. Schematics of the R′ pocket in NPP. (A) Schematic of the transition state and R′ pocket interactions in NPP, based on the crystal structure of PDB entry 2GSU in which AMP was cocrystallized with NPP.[17] Colored magenta is AMP. Colored gray are the Zn^{2+} ions and residues remote from the opening of the pocket to the active site that presumably forms interactions with the nucleoside base. Colored green, orange, aqua, and blue are residues T90, L123, F91, and Y205, respectively, which are located at the mouth of the pocket. (B) Surface representation of the seven residues in the pocket. The colors correspond to the colors in panel A.

describe the effects of successively adding back wild-type residues to this minimal construct. The results provide information about how these residues alone and in combination may contribute to discrimination between different diesterase

dx.doi.org/10.1021/bi4010045 | *Biochemistry* 2013, 52, 9167−9176

Table 1. Distances (in angstroms) of the R′ Pocket Residues from the Phosphoryl Oxygen Atom and 5′-Methylene of AMP[a]

	O	CH_2
L123	4.0	3.7
T90	4.5	3.7
F91	6.5	5.4
Y205	6.6	5.3
Y174	9.2	8.0
E160	11.2	11.6
S155	12.8	10.4

[a]Distances taken from the structure of PDB entry 2GSU.[17]

substrates. Finally, we describe the effects of the mutations on the promiscuous monoesterase reaction, pNPP hydrolysis, results that implicate T90 and L123 as together being responsible for an inhibitory effect on this reaction.

Reconstructing Diesterase Specificity from a R′ Pocket Quadruple Mutant to the Wild-type Enzyme. *L123A/T90S/F91A/Y205A Quadruple Mutant.* The quadruple mutant has the four residues within 7 Å of the 5′-methylene of AMP, F91, L123, Y205, and T90, mutated (Table 1 and Figure 2); each residue was mutated to Ala except, T90, which was mutated to Ser to remove the methyl group but maintain the nucleophilic oxygen. We measured the effects of the mutations with three diesterase substrates that have the same leaving group but different R′ substituents (Chart 1).

The quadruple mutant has k_{cat}/K_M values that are lower than that of wild-type NPP for the hydrolysis of each diester substrate (Table 2 and Figure 3A). For the quadruple mutant, the value of k_{cat}/K_M for the bis-pNPP reaction is reduced by 320-fold, relative to that of the wild-type, and the k_{cat}/K_M values for the bis-pNPP and Me-pNPP reactions are within 1.5-fold of each other (Tables 2 and 3), suggesting that remote favorable interactions with the *p*-nitrophenyl R′ substituent present in wild-type NPP have been eliminated. Furthermore, the value of k_{cat}/K_M for the dT-5′-pNPP reaction of the quadruple mutant is only 28-fold greater than that for the Me-pNPP reaction instead of more than 10^3-fold greater as for the wild-type NPP (Table 2),[a] strongly suggesting that the favorable interactions with this substrate have also been substantially reduced. The remaining 28-fold preference for the 5′-dT R′ group presumably originates from interactions with the polar residues remote from the mouth of the pocket that were not mutated (S155, E160, and Y174 in Figure 2).

Table 2. Rate Constants (k_{cat}/K_M) for Monoesterase ($pNPP^{2-}$) and Diesterase (Me-pNPP, bis-pNPP, and dT-5′-pNPP) Reactions of NPP and Its Mutants[a]

	$pNPP^{2-}$ (M^{-1} s^{-1})	Me-pNPP[b] (M^{-1} s^{-1})	bis-pNPP[b] (M^{-1} s^{-1})	dT-5′-pNPP (M^{-1} s^{-1})
wild-type NPP	1.1	230	2300	$>1.6 \times 10^6$
T90S	3.9	110	1600	3.2×10^5
L123A	5.4	29	2300	1.1×10^6
F91A	2.3	110	1600	4.4×10^5
Y205A	1.1	50	300	2.7×10^5
T90S/L123A	5.6	16	130	3.7×10^4
T90S/F91A/L123A	6.8	13	130	7200
T90S/F91A/L123A/Y205A	5.7	4.7	7.1	130

[a]Values of k_{cat}/K_M were obtained in 0.1 M Tris-HCl (pH 8.0), 0.5 M NaCl, and 100 μM $ZnCl_2$ at 25 °C. The uncertainties for the values of k_{cat}/K_M are within ±20% as estimated by the standard deviations of three repeat measurements for the pNPP reactions of the mutants. Values of k_{cat}/K_M for reactions catalyzed by wild-type NPP are from ref 17. [b]The uncatalyzed hydrolysis rate constants for bis-pNPPand Me-pNPP are very similar, 2.9×10^{-13} and 4.7×10^{-12} M^{-1} s^{-1}, respectively, and thus do not account for the observed differences in k_{cat}/K_M.[15] The uncatalyzed rate of hydrolysis is expected to be similar for dT-5′-pNPP.

The quadruple mutant has a 49-fold lower reactivity with Me-pNPP than wild-type NPP (Table 3), consistent with the model in which some or all of the residues removed participate in hydrophobic interactions with the methyl group directly attached to the phosphoryl group. The results are also consistent with a disruption of the catalytic apparatus. However, as described below (The R' Pocket is Inhibitory with Respect to the Monoesterase Reaction), the observed increase in reactivity of the phosphate monoester substrate upon mutation supports the model with direct interactions. Further support for a dominant effect from direct hydrophobic interactions is described in the following section.

Reintroduction of Y205 into the Pocket: The L123A/T90S/F91A Triple Mutant. Reintroducing Y205 into the R′ pocket, to give the T90S/F91A/L123A triple mutant, gave increases in k_{cat}/K_M of 18- and 55-fold for the bis-pNPP and dT-5′-pNPP reactions, respectively, relative to that of the quadruple mutant but had only a weak effect of 2.8-fold on the Me-pNPP reaction (Figure 3B). These results suggest that Y205 makes remote interactions with the larger diester substituents. No direct interaction between Y205 and AMP is seen in the NPP·AMP cocrystal structure,[17] but it is possible that there are interactions with the thymidine group of dT-5′-pNPP and/or indirect interactions via solvent molecules.

Phylogenetic analysis of the seven classes of NPP reveals that this residue is conserved within all canonical NPPs, despite other differences in the composition of the residues in their pockets and the substrates that they recognize (data not shown). This conservation is consistent with models in which Y205, presumably via its hydrogen bond to a Zn^{2+} ligand (D54 in NPP) (Figure S2 of the Supporting Information), plays an evolutionarily significant role in ordering the active site. However, the decrease of only 3−5-fold for the Me-PNPP reaction upon removal of the Y205 side chain in the wild-type background or triple-mutant background [to give the quadruple mutant (Tables 2 and 3)] suggests that any effect on the overall active site function upon removal of this residue is modest.

Reintroduction of F91: The T90S/L123A Double Mutant. There is a 5-fold increase in k_{cat}/K_M for the dT-5′-pNPP reaction upon reintroduction of F91 to give the double mutant, T90S/L123A (Figure 3B and Table 2). In contrast, reintroduction of F91 in the double mutant results in a <2-fold increase in k_{cat}/K_M for the Me-pNPP and bis-pNPP reactions (Figure 3B and Table 2), and similar weak effects are seen from the removal of this residue to give the F91A single mutant (Tables 2 and 3).

Inspection of the NPP·AMP cocrystal structure suggests that F91 may interact with the ribose ring of nucleosides to provide its favorable effect for the reaction of dT-5′-pNPP.[17] F91 is 5.4 Å from the 5′-methylene group of AMP and so would not have been predicted to directly interact with the methyl group of Me-pNPP. The *p*-nitrophenyl substituent of bis-pNPP could interact but apparently does not, presumably because such an

dx.doi.org/10.1021/bi4010045 | *Biochemistry* 2013, 52, 9167−9176

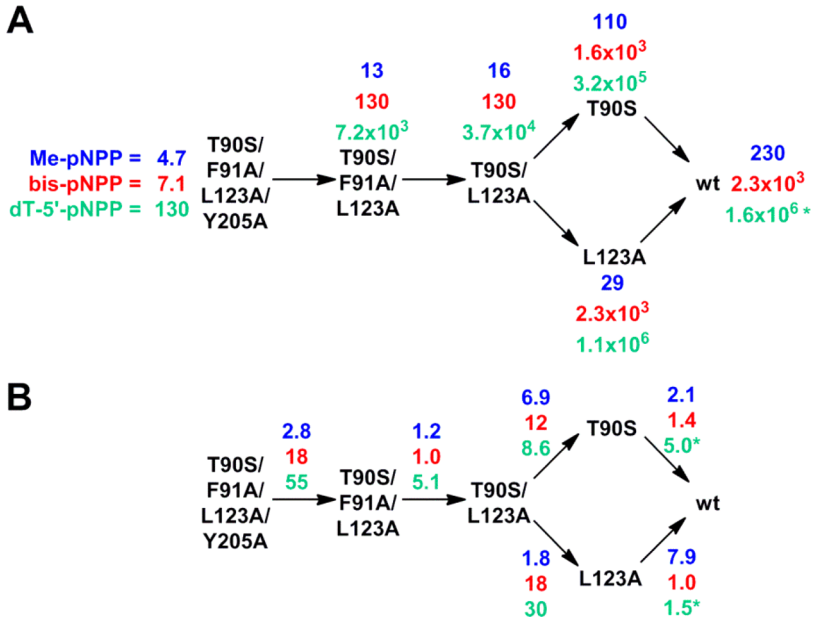

Figure 3. Values of k_{cat}/K_M (A) and fold differences (B) in the mutant and wild-type NPPs with the three different diester substrates, Me-pNPP, bis-pNPP, and dT-5′-pNPP (color coded). (A) Values of k_{cat}/K_M for the mutant and wild-type NPPs with different diester substrates. (B) Fold increases in these values of the diesterase reactions as one moves from the most mutated enzyme, T90S/F91A/L123A/Y205A, to the wild-type enzyme. The numbers are color-coded as in panel A. The chemical step is not rate-limiting for the reaction of wild-type NPP with dT-5′-pNPP, so that the observed effects of the mutations on this reaction presumably underestimate the overall effects on binding and stability of the chemical transition state, as denoted with asterisks.[17]

Table 3. k_{rel} Values for Monoesterase ($pNPP^{2-}$) and Diesterase (Me-pNPP, bis-pNPP, and dT-5′-pNPP) Reactions of NPP and Its Mutants[a]

	$pNPP^{2-}$	Me-pNPP	bis-pNPP	dT-5′-pNPP
wild-type NPP	(1)	(1)	(1)	(1)
T90S	0.28	2.1	1.4	5.0*
L123A	0.20	7.9	1.0	1.5*
F91A	0.48	2.1	1.4	3.6*
Y205A	1.0	4.6	7.7	5.9*
T90S/L123A	0.20	14	18	43*
T90S/F91A/L123A	0.16	18	18	220*
T90S/F91A/L123A/Y205A	0.19	49	320	12000*

[a] $k_{rel} = (k_{cat}/K_M)_{wt}/(k_{cat}/K_M)_{mutant}$. Because the chemical step is not rate-limiting for the reaction of dT-5′-pNPP with the wild type, the measured rate constants for the mutants most likely represent underestimates of the true effects of these mutations on the chemical transition state of this reaction and are denoted with asterisks.

interaction would not be favorable or because of geometric constraints from the binding pocket or aromatic ring.

A Double-Mutant Cycle To Evaluate the Contributions from T90 and L123. Comparison of the double mutant, T90S/L123A, to wild-type NPP reveals a 14-fold decrease in the k_{cat}/K_M value of the Me-pNPP reaction (Table 3). Mutating L123 to alanine in the wild-type and T90S backgrounds gave similar effects of 7.9- and 6.9-fold, respectively, and the effect of mutating T90 to serine also had similar 2.1- and 1.8-fold effects in the wild-type and L123A backgrounds, respectively (Figure 3B). Thus, each residue interacts favorably and energetically independently with the methyl substituent, with the leucine residue providing a larger contribution.

In contrast, there is coupling between T90 and L123 in the bis-pNPP reaction. There is an 18-fold decrease in the k_{cat}/K_M for the double mutant compared to that of wild-type NPP (Table 3); however, removing the side chain of either residue alone has only a weak effect of <2-fold, whereas removal of the second residue, whichever it is, gives a >10-fold effect (Figure 3B). The simplest model to account for these results is that in which the *p*-nitrophenyl R′ group can interact with either side chain but not both simultaneously, although other, more complex explanations are also possible, including favorable interactions with the second residue added that are offset by geometrical restrictions that introduce unfavorable remote interactions or prevent remote favorable interactions. Coupling cannot be assayed with dT-5′-pNPP because the chemical step is not rate-limiting for wild-type NPP.[17]

The R′ Pocket Is Inhibitory with Respect to the Monoesterase Reaction. We hypothesized that hydrophobic residues that aid recognition of hydrophobic R′ substituents might prevent optimal solvation of a partially negatively charged oxygen atom at this position as would be present in the transition state for reaction of a phosphate monoester substrate (Figure 2). If so, removal of these residues might increase the monoesterase activity.

We first had to ensure that the low, observed promiscuous monoesterase activity measured with pNPP arose from the NPP active site and not from a contaminant. A simple but strong prediction for promiscuous and cognate reactions arising from a single active site is that the two reactions will follow the same inhibition profile for a common active site ligand (under subsaturating and identical buffer conditions).[10,11,14−17] We therefore determined the inhibition constants for vanadate or tungstate for the diesterase and monoesterase reactions for wild-type NPP and for each of the mutants studied (Figure 4 and Table 4). The choice of the inhibitor used for each mutant was based upon which inhibitor, vanadate or tungstate, had the lowest and thus most easily measurable inhibition constant. For each NPP mutant, the same inhibition constant was obtained,

dx.doi.org/10.1021/bi4010045 | *Biochemistry* 2013, 52, 9167−9176

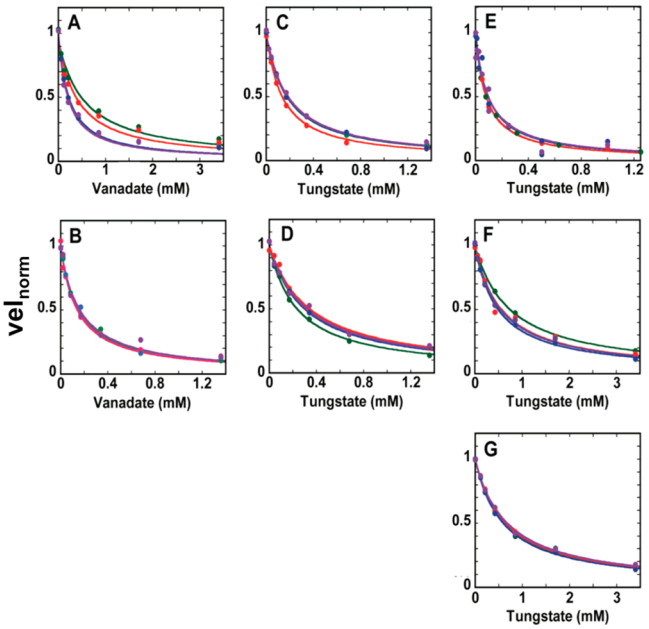

Figure 4. Comparison of the inhibition by tungstate or vanadate of the monoesterase ($pNPP^{2-}$, purple) and diesterase reactions (Me-pNPP, blue; bis-pNPP, red; dT-5′-pNPP, green) for each of the NPP mutants: (A) T90S, (B) L123A, (C) F91A, (D) Y205A, (E) T90S/L123A, (F) T90S/F91A/L123A, and (G) T90S/F91A/L123A/Y205A. The choice of inhibitor was determined by which one bound most strongly to each mutant. Activity was normalized by the observed reaction in the absence of an inhibitor, corresponding to a normalized velocity (*y*-axis) of 1, and the lines are nonlinear least-squares fits for competitive inhibition. The curves were fit to a fixed end point of zero. Inhibition constants and errors are listed in Table S2 of the Supporting Information.

within error, for all of its reactions. This observation provided evidence against catalysis by a contaminating activity and allowed us to investigate the phosphate monoesterase activity of the mutants.

Removal of the T90 methyl group or the L123 side chain gave an increase of 4−5-fold in the monoesterase activity, and an increase of up to 7-fold was observed for the mutants studied (Table 2, triple mutant). In contrast, mutation of Y205 or F91 gave at most 2-fold increases in phosphate monoesterase activity.

To improve our understanding of the origin of the enhancement of monoesterase activity, we examined a double-mutant cycle for T90 and L123, the removal of which enhances monoesterase activity (Figure 5). Mutation of either

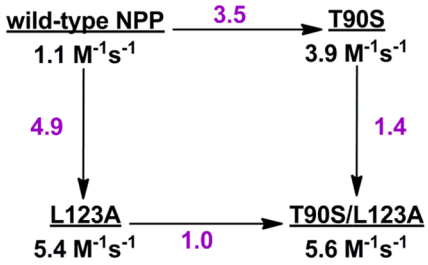

Figure 5. Double-mutant cycle between T90S/L123A and wild-type NPP with the monoester ($pNPP^{2-}$) reaction. Colored black below the enzyme names are the k_{cat}/K_M values for each enzyme. Colored purple is the fold increase in the k_{cat}/K_M values of the two enzymes connected by the arrow.

residue increased monoesterase activity to nearly the level of the double mutant; i.e., the second mutation had a negligible effect. The simplest explanation for these results is that removal of either nearby side chain allows access by water that is sufficient to provide solvation interaction energies similar to those in bulk solvent.

The Quadruple Mutant Provides the Same Rate Enhancement for Phosphate Diester and Monoester Reactions. Our data indicate that the R′ pocket is a major specificity determinant in NPP. Once favorable and unfavorable interactions from the R′ binding pocket have been removed, by mutation and by minimization of the R′ substituent, this quadruple mutant does not distinguish between substrates of two different reaction classes, phosphate monoesters and phosphate diesters, giving k_{cat}/K_M values for pNPP dianion ($pNPP^{2-}$) and Me-pNPP monoanion hydrolysis within 1.5-fold of one another (Figure 6 and Table 2). The 79-fold preferential reactivity of wild-type NPP with pNPP monoanion ($pNPP^{-}$) (where R′ = H) over $pNPP^{2-}$ is eliminated in the quadruple mutant (Figure 6 and the Supporting Information), again consistent with the removal of interactions that are deleterious for an oxyanion in the R′ site. The uncatalyzed hydrolysis reactions of Me-pNPP and $pNPP^{2-}$ are similar, and their k_{cat}/K_M values with the quadruple mutant are nearly identical, indicating that this NPP mutant catalyzes these distinct

Table 4. Inhibition Constants[a] for Monoesterase ($pNPP^{2-}$) and Diesterase (Me-pNPP, bis-pNPP, and dT-5′-pNPP) Reactions Catalyzed by Wild-Type NPP and Its Different Mutants

	K_I (μM)					
	$pNPP^{2-}$	Me-pNPP	bis-pNPP	dT-5′-pNPP	average	standard deviation
			Tungstate			
F91A	174	135	175	184	167	19
Y205A	319	298	343	236	299	40
T90S/L123A	109	95	80	82	92	13
T90S/F91A/L123A	547	494	564	742	587	93
T90S/F91A/L123A/Y205A	680	591	652	624	637	33
			Vanadate			
T90S	200	216	404	541	340	140
L123A	162	159	141	153	154	8

[a]Values for the inhibition constants were obtained with 0.1 M Tris-HCl (pH 8.0), 0.5 M NaCl, and 100 μM $ZnCl_2$ at 25 °C. The choice of inhibitor was based on the one with the lowest initial inhibition constant for the dT-5′-pNPP reaction.

dx.doi.org/10.1021/bi4010045 | *Biochemistry* 2013, 52, 9167−9176

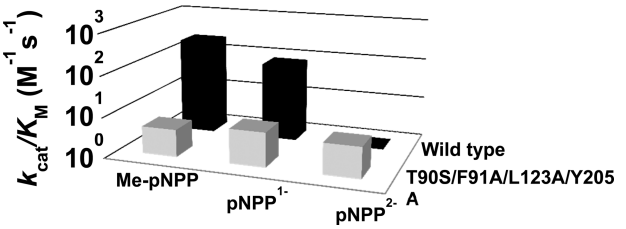

Figure 6. Quadruple mutant, T90S/F91A/L123A/Y205A, is a generalist enzyme. The k_{cat}/K_M values for the diester, Me-pNPP, monoester monoanion, $pNPP^-$, and monoester dianion, $pNPP^{2-}$, reactions of the quadruple mutant are 4.7, 5, and 5.7 M^{-1} s^{-1}, respectively. The rate constant for monoanion $pNPP^-$ is listed with only one significant figure as it was obtained from a pH−rate profile that extends only slightly below the pK_a of pNPP (Supporting Information).

reactions with the nearly the same rate enhancement (Figure 6 and Table 5).

Table 5. Rate Enhancements $[(k_{cat}/K_M)/k_w]$ for the Monoester ($pNPP^{2-}$) and Diester (Me-pNPP) Reactions of NPP and Its Mutants[a]

	$pNPP^{2-}$	Me-pNPP	Me-pNPP/$pNPP^{2-}$
wild-type NPP	3.3×10^{10}	4.9×10^{13}	1500
T90S	1.3×10^{11}	2.4×10^{13}	180
L123A	1.8×10^{11}	6.3×10^{12}	35
F91A	7.7×10^{10}	2.3×10^{13}	300
Y205A	3.7×10^{10}	1.1×10^{13}	300
T90S/L123A	1.9×10^{11}	3.3×10^{12}	17
T90S/F91A/L123A	2.3×10^{11}	2.8×10^{12}	12
T90S/F91A/L123A/Y205A	1.9×10^{11}	1.0×10^{12}	5.3

[a]The Me-pNPP/$pNPP^{2-}$ ratio is the ratio of rate enhancement $[(k_{cat}/K_M)/k_w]$ for the diesterase and monoesterase reactions of the mutants. The k_w values for $pNPP^{2-}$ and Me-pNPP are 3.0×10^{-11} and 4.7×10^{-12} M^{-1} s^{-1}, respectively.[15,39]

CONCLUSIONS

Previous work has shown that nucleotide pyrophosphatase/phosphodiesterase (NPP) exhibits a preference for the hydrolysis of phosphate diesters over phosphate monoesters.[17] The observed reaction specificity of 10^6-fold was reduced by $>10^3$-fold when the size of the substituent on the transferred phosphoryl group of phosphate diester substrates was reduced to a methyl group (Figure 7).[17] Here we show additional specificity contributions from the R′ binding pocket for this substituent that give an additional ∼250-fold decrease in specificity (Figure 8).

Figure 8 summarizes the effects of truncating the side chains of the four residues at the mouth of the R′ pocket of NPP. There is a progressive decrease in diesterase activity, with larger effects for more reactive substrates that have larger R′ groups, but even the reaction of the diester substrate containing only a methyl R′ substituent is affected. Conversely, the monoesterase activity with pNPP increases across this series, though more modestly. Overall, these four residues, T90, F91, L123A, and Y205, enhance specificity both through favorable interactions with the R′ substituent and by unfavorable interactions with the unesterified, negatively charged phosphoryl oxygen atom of the monoesterase substrate.

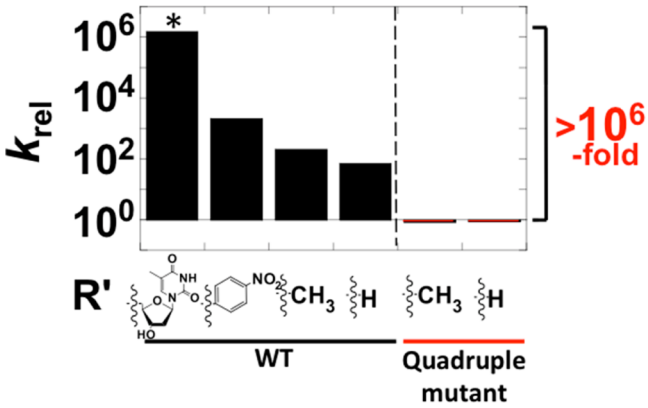

Figure 7. Relative diesterase vs monoesterase reactivity for a series of diester substrates with wild-type NPP and the quadruple mutant, T90S/F91A/L123A/Y205A. $k_{rel} = (k_{cat}/K_M)_{diester}/(k_{cat}/K_M)_{pNPP\ dianion}$, and the pNPP monoanion, $pNPP^-$, is considered diester-like in this series as it likely reacts without the transfer of a proton to the leaving group oxygen. The asterisk denotes that the dT-5′-pNPP diesterase chemical step is not rate-limiting. Values for k_{cat}/K_M are from Table 2.

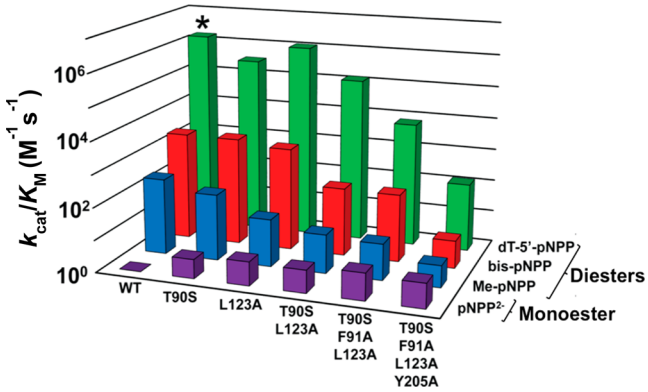

Figure 8. Plot of k_{cat}/K_M values for the monoesterase ($pNPP^{2-}$) and three diesterase (Me-pNPP, bis-pNPP, and dT-5′-pNPP) reactions measured with each of the five mutants. Wild-type NPP k_{cat}/K_M values, from this work and ref 17, are plotted for comparison to those of the mutants. The asterisk denotes that the chemical step is not rate-limiting for the reaction. Values of k_{cat}/K_M are from Table 2.

More detailed consideration of the relative effects of the mutations on the different reactions reveals multiple underlying origins, likely including direct interactions with the carbon unit directly esterified to the nonleaving group phosphoryl oxygen, more remote direct interactions, and indirect effects on the ability to make certain remote interactions. In addition, our results suggest a modest catalytic role of the conserved Y205. Y205 donates a hydrogen bond to one of the Zn^{2+} ligands, which may help organize the Zn^{2+} bimetallo center or orient this center with respect to the threonine nucleophile (Figure S2 of the Supporting Information).

The quadruple mutant with the proximal R′ interactions removed exhibits k_{cat}/K_M values within 2-fold of each other for diesterase (Me-pNPP) and monoesterase ($pNPP^{2-}$) reactions (Figure 8 and Table 2), and the rate enhancements for these reactions are within 5-fold of each other (Table 5). What remains in the active site is the Zn^{2+} bimetallo motif with a set of ligands that is conserved throughout the main branch of the alkaline phosphatase superfamily[9] and N111.[17] Preliminary experiments suggest that removal of N111 has a similar effect on the monoesterase and diesterase reactions (F. Sunden, H.

dx.doi.org/10.1021/bi4010045 | Biochemistry 2013, 52, 9167−9176

Wiersma-Koch, and D. Herschlag, unpublished results). The NPP Zn^{2+} bimetallo motif likely provides similar catalysis for the phosphate di- and monoester reactions.

IMPLICATIONS AND FUTURE DIRECTIONS

We naively might have expected a preference for the reaction of our minimal NPP construct containing the positively charged zinc bimetallo cluster with the more highly charged monoester, a preference that is not observed (Table 5 and Figure 7). It is possible that the NPP Zn^{2+} bimetallo site is tuned to favor reaction with diesters. As the direct Zn^{2+} ligands are fully conserved between phosphate diesterases and monoesterases in the AP superfamily,[19,34] features of the scaffold surrounding the Zn^{2+} ions and their ligands would have to be involved in such tuning.[35] Whether this tuning model holds or whether the bimetallo core unexpectedly has near-equal catalytic power toward both substrate classes can be tested by comparing the reactivities of minimal monoesterase and diesterase constructs derived from alkaline phosphatase superfamily members. These results will have implications both for how these enzymes have evolved and for what protein features need to be and can be varied toward the important goal of engineering and re-engineering enzymes with novel and useful catalytic functions.

Jensen proposed that broadly specific enzymes could have played key roles in metabolism in early, primitive systems,[36] and our AP superfamily minimal mutant fits the strict definition of a "generalist" enzyme. However, the k_{cat}/K_M values of the NPP quadruple mutant are very low compared to values for highly evolved modern-day enzymes, even with the activated leaving groups used in this study (Chart 1 and Figure 8), raising the question of whether such an enzyme could have provided sufficient catalysis to yield a selective advantage.

A second basic evolutionary question is also highlighted by the observation that the Zn^{2+} bimetallo core alone provides an enormous rate enhancement of $\sim 10^{11}$-fold for reactions of both phosphate monoester and phosphate diester substrates (Table 5), a rate enhancement that rivals and indeed exceeds that observed for many modern-day, fully evolved enzymes.[37] How did catalysis of extremely difficult reactions get started? Proposals include early life at high temperatures, initial use of (very) activated substrates, and evolution from enzymes that catalyzed other, easier reactions.[38] Extant AP superfamily members catalyze only phosphoryl and sulfuryl transfer reactions, reactions that, with unactivated leaving groups, have half-lives greater than the lifetime of the universe in solution.

While these evolutionary mysteries remain, our minimal mutant provides a measure of the extent of catalysis that can be provided from the metal ion core alone. In addition, deep dissection and deconstruction of cognate and promiscuous enzyme activities may help guide current efforts in enzyme design and reengineering toward the goals of better understanding enzyme function and producing highly efficient and specific catalysts for reactions of biomedical and industrial interest.

ASSOCIATED CONTENT

Supporting Information

Discussions of the pH dependencies of the mutants, the sequence of the MBP-$NPP_{strepII}$ construct used in this study, a schematic of the hydrogen bond between Y205 and D54, graphs of the pH dependencies for the reaction of T90S/F91A/L123A/Y205A with pNPP and Me-pNPP, and a graph of the pH dependencies of all the mutants with pNPP between pH 7 and 9. This material is available free of charge via the Internet at http://pubs.acs.org.

AUTHOR INFORMATION

Corresponding Author

*Department of Biochemistry, Stanford University School of Medicine, Stanford, CA 94305. E-mail: herschla@stanford.edu. Telephone: (650) 723-9442. Fax: (650) 723-6783.

Funding

This work was supported by a grant from the National Institutes of Health (NIH) to D.H. (GM64798). H.W.-K. was supported in part by NIH Training Grant R1GM064798.

Notes

The authors declare no competing financial interest.

ACKNOWLEDGMENTS

We thank members of the Herschlag lab for critical discussions and comments on the manuscript. We thank Jonathan Lassila, Alan Barber, Michael Hicks, and Patsy Babbitt for useful discussions and use of unpublished results.

ABBREVIATIONS

AP, alkaline phosphatase; NPP, nucleotide pyrophosphatase/phosphodiesterase; MBP, maltose binding protein; AMP, adenosine monophosphate; R′ pocket, NPP substituent binding pocket; Me-pNPP, methyl 4-nitrophenyl phosphate; pNPP, 4-nitrophenyl phosphate; bis-pNPP, bis-4-nitrophenyl phosphate; dT-5′-pNPP, thymidine 5′-monophosphate 4-nitrophenyl ester; wt, wild type; PDB, Protein Data Bank.

ADDITIONAL NOTE

[a]The chemical step is not rate-limiting for the reaction of wild-type NPP with dT-5′-pNPP,[17] so that the observed effects of the mutations of this reaction underestimate the overall effects on the binding and stability of the chemical transition state.

REFERENCES

(1) O'Brien, P. J., and Herschlag, D. (1999) Catalytic promiscuity and the evolution of new enzymatic activities. *Chem. Biol. 6*, R91−R105.

(2) Khersonsky, O., and Tawfik, D. S. (2010) Enzyme promiscuity: A mechanistic and evolutionary perspective. *Annu. Rev. Biochem. 79*, 471−505.

(3) James, L. C., and Tawfik, D. S. (2003) Conformational diversity and protein evolution: A 60-year-old hypothesis revisited. *Trends Biochem. Sci. 28*, 361−368.

(4) Gerlt, J. A., Babbitt, P. C., and Rayment, I. (2005) Divergent evolution in the enolase superfamily: The interplay of mechanism and specificity. *Arch. Biochem. Biophys. 433*, 59−70.

(5) Yew, W. S., Akana, J., Wise, E. L., Rayment, I., and Gerlt, J. A. (2005) Evolution of enzymatic activities in the orotidine 5′-monophosphate decarboxylase suprafamily: Enhancing the promiscuous D-arabino-hex-3-ulose 6-phosphate synthase reaction catalyzed by 3-keto-L-gulonate 6-phosphate decarboxylase. *Biochemistry 44*, 1807−1815.

(6) Wise, E. L., Yew, W. S., Akana, J., Gerlt, J. A., and Rayment, I. (2005) Evolution of enzymatic activities in the orotidine 5′-monophosphate decarboxylase suprafamily: Structural basis for catalytic promiscuity in wild-type and designed mutants of 3-keto-L-gulonate 6-phosphate decarboxylase. *Biochemistry 44*, 1816−1823.

(7) Elias, M., and Tawfik, D. S. (2011) Divergence and Convergence in Enzyme Evolution: Parallel Evolution of Paraoxonases from Quorum-quenching Lactonases. *J. Biol. Chem. 287*, 11−20.

(8) Gerlt, J. A., and Babbitt, P. C. (2001) Divergent evolution of enzymatic function: Mechanistically diverse superfamilies and functionally distinct suprafamilies. *Annu. Rev. Biochem. 70*, 209−246.
(9) Galperin, M. Y., Bairoch, A., and Koonin, E. V. (1998) A superfamily of metalloenzymes unifies phosphopentomutase and cofactor-independent phosphoglycerate mutase with alkaline phosphatases and sulfatases. *Protein Sci. 7*, 1829−1835.
(10) van Loo, B., Jonas, S., Babtie, A. C., Benjdia, A., Berteau, O., Hyvonen, M., and Hollfelder, F. (2010) An efficient, multiply promiscuous hydrolase in the alkaline phosphatase superfamily. *Proc. Natl. Acad. Sci. U.S.A. 107*, 2740−2745.
(11) Babtie, A., Bandyopadhyay, S., Olguin, L., and Hollfelder, F. (2009) Efficient Catalytic Promiscuity for Chemically Distinct Reactions. *Angew. Chem., Int. Ed. 48*, 3692−3694.
(12) Bihani, S. C., Das, A., Nilgiriwala, K. S., Prashar, V., Pirocchi, M., Apte, S. K., Ferrer, J., and Hosur, M. V. (2011) X-Ray Structure Reveals a New Class and Provides Insight into Evolution of Alkaline Phosphatases. *PLoS One 6*, e22767.
(13) Kim, A., Benning, M. M., OkLee, S., Quinn, J., Martin, B. M., Holden, H. M., and Dunaway-Mariano, D. (2011) Divergence of chemical function in the alkaline phosphatase superfamily: Structure and mechanism of the P-C bond cleaving enzyme phosphonoacetate hydrolase. *Biochemistry 50*, 3481−3494.
(14) Jonas, S., Loo, B., Hyvönen, M., and Hollfelder, F. (2008) A New Member of the Alkaline Phosphatase Superfamily with a Formylglycine Nucleophile: Structural and Kinetic Characterisation of a Phosphonate Monoester Hydrolase/Phosphodiesterase from *Rhizobium leguminosarum*. *J. Mol. Biol. 348*, 120−136.
(15) Lassila, J. K., and Herschlag, D. (2008) Promiscuous Sulfatase Activity and Thio-Effects in a Phosphodiesterase of the Alkaline Phosphatase Superfamily. *Biochemistry 47*, 12853−12859.
(16) O'Brien, P., and Herschlag, D. (1998) Sulfatase activity of *E. coli* alkaline phosphatase demonstrates a functional link to arylsulfatases, an evolutionarily related enzyme family. *J. Am. Chem. Soc. 120*, 12368−12370.
(17) Zalatan, J. G., Fenn, T. D., Brunger, A. T., and Herschlag, D. (2006) Structural and Functional Comparisons of Nucleotide Pyrophosphatase/Phosphodiesterase and Alkaline Phosphatase: Implications for Mechanism and Evolution. *Biochemistry 45*, 9788−9803.
(18) Zalatan, J. G., Fenn, T. D., and Herschlag, D. (2008) Comparative Enzymology in the Alkaline Phosphatase Superfamily to Determine the Catalytic Role of an Active-Site Metal Ion. *J. Mol. Biol. 384*, 1174−1189.
(19) Bobyr, E., Lassila, J. K., Wiersma-Koch, H. I., Fenn, T. D., Lee, J. J., Nikolic-Hughes, I., Hodgson, K. O., Rees, D. C., Hedman, B., and Herschlag, D. (2012) High-Resolution Analysis of Zn^{2+} Coordination in the Alkaline Phosphatase Superfamily by EXAFS and X-ray Crystallography. *J. Mol. Biol. 415*, 102−117.
(20) O'Brien, P. J., and Herschlag, D. (2002) Alkaline Phosphatase Revisited: Hydrolysis of Alkyl Phosphates. *Biochemistry 41*, 3207−3225.
(21) Stefan, C., Jansen, S., and Bollen, M. (2005) NPP-type ectophosphodiesterases: Unity in diversity. *Trends Biochem. Sci. 30*, 542−550.
(22) Duan, J., Wu, J., Cheng, Y., and Duan, R. (2010) Understanding the molecular activity of alkaline sphingomyelinase (NPP7) by computer modeling. *Biochemistry 49*, 9096−9105.
(23) Mackenzie, N. C. W., Huesa, C., Rutsch, F., and MacRae, V. E. (2012) New insights into NPP1 function: Lessons from clinical and animal studies. *Bone 51*, 961−968.
(24) Cheng, Y., Wu, J., Hertervig, E., Lindgren, S., Duan, D., Nilsson, A., and Duan, R. (2007) Identification of aberrant forms of alkaline sphingomyelinase (NPP7) associated with human liver tumorigenesis. *Br. J. Cancer 97*, 1441−1448.
(25) Andrade, C. M., Wink, M. R., Margis, R., Borojevic, R., Battastini, A. M., and Guma, F. C. (2009) Activity and expression of ecto-nucleotide pyrophosphate/phosphodiesterases in a hepatic stellate cell line. *Mol. Cell. Biochem. 325*, 179−185.
(26) Zhang, Y., Cheng, Y., Hansen, G. H., Niels-Christiansen, L., Koentgen, F., Ohlsson, L., Nilsson, A., and Duan, R. (2011) Crucial role of alkaline sphingomyelinase in sphingomyelin digestion: A study on enzyme knockout mice. *J. Lipid Res. 52*, 771−781.
(27) Kawaguchi, M., Okabe, T., Okudaira, S., Hanaoka, K., Fujikawa, Y., Terai, T., Komatsu, T., Kojima, H., Aoki, J., and Nagano, T. (2011) Fluorescence Probe for Lysophospholipase C/NPP6 Activity and a Potent NPP6 Inhibitor. *J. Am. Chem. Soc. 133*, 12021−12030.
(28) Clair, T., Lee, H. Y., Liotta, L. A., and Stracke, M. L. (1997) Autotaxin is an exoenzyme possessing 5′-nucleotide phosphodiesterase/ATP pyrophosphatase and ATPase activities. *J. Biol. Chem. 272*, 996−1001.
(29) Saunders, L. P., Cao, W., Chang, W. C., Albright, R. A., Braddock, D. T., and de La Cruz, E. M. (2011) Kinetic analysis of autotaxin reveals substrate-specific catalytic pathways and a mechanism for lysophosphatidic acid distribution. *J. Biol. Chem. 286*, 30130−30141.
(30) Voss, S., and Skerra, A. (1997) Mutagenesis of a flexible loop in streptavidin leads to higher affinity for the Strep-tag II peptide and improved performance in recombinant protein purification. *Protein Eng. 10*, 975−982.
(31) Skerra, A., and Schmidt, T. G. (2000) Use of the Strep-Tag and streptavidin for detection and purification of recombinant proteins. *Methods Enzymol. 326*, 271−304.
(32) Witte, C., Noël, L., Gielbert, J., Parker, J., and Romeis, T. (2004) Rapid one-step protein purification from plant material using the eight-amino acid StrepII epitope. *Plant Mol. Biol. 55*, 135−147.
(33) Diezel, W., Kopperschläger, G., and Hofmann, E. (1972) An improved procedure for protein staining in polyacrylamide gels with a new type of Coomassie Brilliant Blue. *Anal. Biochem. 48*, 617−620.
(34) Gijbers, R., Ceulemans, H., Stalmans, W., and Bollen, M. (2001) Structural and catalytic similarities between nucleotide pyrophosphatases/phosphodiesterases and alkaline phosphatases. *J. Biol. Chem. 276*, 1361−1368.
(35) Xu, X., Qin, X. Q., and Kantrowitz, E. R. (1994) Probing the role of histidine-372 in zinc binding and the catalytic mechanism of *Escherichia coli* alkaline phosphatase by site-specific mutagenesis. *Biochemistry 33*, 2279−2284.
(36) Jensen, R. A. (1976) Enzyme recruitment in evolution of new function. *Annu. Rev. Microbiol. 30*, 409−425.
(37) Wolfenden, R., and Snider, M. J. (2001) The depth of chemical time and the power of enzymes as catalysts. *Acc. Chem. Res. 34*, 938−945.
(38) Wolfenden, R. (2011) Benchmark reaction rates, the stability of biological molecules in water, and the evolution of catalytic power in enzymes. *Annu. Rev. Biochem. 80*, 645−667.
(39) Benkovic, S. J., and Benkovic, P. A. (1966) Studies of Sulfate Esters. I. Nucleophilic reactions of amines with *p*-Nitrophenyl Sulfate. *J. Am. Chem. Soc. 88*, 5504−5511.